Orientational correlations and hydrogen bonding in liquid hydrogen chloride

C. Andreani, M. A. Ricci, M. Nardone, F. P. Ricci, and A. K. Soper

Citation: The Journal of Chemical Physics **107**, 214 (1997); doi: 10.1063/1.474368
View online: http://dx.doi.org/10.1063/1.474368
View Table of Contents: http://scitation.aip.org/content/aip/journal/jcp/107/1?ver=pdfcov
Published by the AIP Publishing

Orientational correlations and hydrogen bonding in liquid hydrogen chloride

C. Andreani
Dipartimento di Fisica, Universitá degli Studi di Tor Vergata, Istituto Nazionale di Fisica della Materia, Unita' di Roma Tor Vergata, Via della Ricerca Scientifica 1, 00133 Rome, Italy

M. A. Ricci, M. Nardone, and F. P. Ricci
Dipartimento di Fisica ''E. Amaldi,'' Universitá degli Studi di Roma Tre, Istituto Nazionale di Fisica della Materia, Unitá di Roma Tre, Via della Vasca Navale 84, 00146 Rome, Italy

A. K. Soper[a)]
ISIS Facility, Rutherford Appleton Laboratory, Chilton, Didcot, Oxfordshire, OX11 0QX, United Kingdom

(Received 21 January 1997; accepted 27 March 1997)

Neutron diffraction data, obtained by employing the hydrogen isotope substitution technique, on orthobaric hydrogen chloride at two state points are presented. The site-site radial distribution functions are derived from these data and are compared with similar results obtained previously for hydrogen iodide and hydrogen bromide. Comparison of the measured hydrogen-hydrogen and chlorine-hydrogen radial distribution functions with those derived assuming uncorrelated orientations demonstrates the presence of strong orientational correlations between first neighboring HCl molecules at both states. An analysis of molecular configurations compatible with the experimental data as generated by a Monte Carlo simulation routine is used to discuss the extent of hydrogen bonding in liquid HCl. © *1997 American Institute of Physics.* [S0021-9606(97)51125-1]

I. INTRODUCTION

Neutron diffraction studies aimed to look at orientational correlations among molecules in a liquid have always been limited by the intrinsic difficulty that the response of the system to the probe is a weighted sum of all the independent site-site correlation functions.[1] It is nevertheless now well established that for hydrogen containing liquids one can exploit the large change in the coherent neutron scattering length existing between H and D isotopes by performing neutron diffraction experiments with Isotopic H/D Substitution (NDIS)[2] and thus extract three independent site-site correlation functions. In simple molecular fluids, such as the hydrogen halides, this technique allows the extraction of the whole set of independent functions.[3,4] In these molecular liquids the availability of the whole set of site-site correlation functions is ''per se'' of great help in understanding the orientational correlations, although a detailed knowledge of the entire angular pair correlation function cannot be achieved. As a matter of fact the angular pair correlation function contains more information than contained in the set of site-site correlation functions, since the latter are averages of the angular pair correlation function over the molecular orientations, keeping the site-site distance fixed.[5] Deeper insight into the orientational correlations can be obtained only by interpreting the experimental data along with appropriate computer simulations, such as Reverse Monte Carlo,[6] Molecular Dynamics[7] or the recently developed Empirical Potential Monte Carlo Simulation[8] (EPMC).

Molecular liquids composed of hydrogen halides have two features in common, which can be of help in understanding the orientational correlations. First the center of mass is approximately coincident with the halide atom, which means that the halide-halide correlation function extracted from the diffraction experiment coincides with the centers of mass radial distribution function to a good approximation. Second, the hard core part of the intermolecular potential is almost spherically symmetric: therefore the orientational correlations can be interpreted in terms of electrostatic multipolar interactions and hydrogen bond formation. In particular the anisotropy of the intermolecular potential is strongly varying within the halide series, since the dipolar contribution decreases when going from hydrogen fluoride to hydrogen iodide, while the quadrupole contribution increases.[5,9]

Three neutron diffraction studies[10–12] have already been published on hydrogen chloride. All of them report experimental data taken at a reactor source on the orthobaric liquid around room temperature, and the density dependence along a supercritical isotherm is also investigated in the last paper. The former[10] and the last[12] studies have been performed without exploiting the isotopic substitution, therefore only the neutron weighted radial correlation function of the liquid has been derived. In both cases the authors ascribe the peak at about 2.6 Å, in the radial distribution function of room temperature hydrogen chloride, to the existence of hydrogen bonds in the liquid state. This peak is still visible, at about 2.3 Å, at the highest density on the supercritical isotherm.[12] In the second study[11] the three site-site correlation functions were determined for the first time, using the isotopic substitution technique, but only a limited Q-range was available. In this case it was possible to give an estimate of positions and amplitudes of the peaks in the three site-site radial distribution functions, and, from a comparison with computer simulation results, the data revealed the distinctive role of

[a)]Also at: Department of Physics and Astronomy, University College London, Gower Street. London WC1E 6BT, United Kingdom.

 0021-9606/97/107(1)/214/8/$10.00

multipolar forces in determining the structure of the liquid.

For the simulation work a series of pairwise additive model potentials were used.[13–15] The comparison of these simulations with the experimental data of Soper and Egelstaff[11] suggests that better overall agreement between experimental and simulated pair correlation functions is obtained when electrostatic forces between appropriate fractional charges are included.[14] Gutwerk *et al.*[15] have recently tested several such models against the density dependence of the neutron weighted radial correlation function at supercritical temperatures. These authors propose a new effective potential model, which reproduces the trend of the experimental data of Ref. 12. Their calculated $g_{\mathrm{ClCl}}(r)$ resembles the distribution of an atomic liquid and the H-bond peak shows a clear density dependence.

In the present paper we will describe a detailed NDIS study performed on liquid HCl at two thermodynamic states, one close to the triple point, i.e., at $T=194$ K (where $\rho=0.0196$ molecules/Å^3) and the other close to the critical temperature, i.e., at $T=313$ K (where $\rho=0.01134$ molecules/Å^3).[16] The aim of the present work is twofold, first to investigate the orientational correlations between neighboring molecules in this liquid, comparing the results with the other hydrogen halides (i.e., HI[3] and HBr[4]) at the same reduced temperature ($T^*=T/T_c=0.6$) and second to assess the degree of hydrogen bonding in HCl.

II. EXPERIMENTAL PROCEDURE AND DATA REDUCTION

A. Experiment

The NDIS experiments on HCl, as previous ones on the other hydrogen halides,[3,4] were performed using the SANDALS diffractometer installed at the pulsed neutron source, ISIS, at Rutherford Appleton Laboratory. In this diffractometer, an incoming white neutron beam impinges on a sample placed at a distance L_o from the moderator, and neutrons diffracted from the sample are recorded downstream by scintillation detectors located in a wide angular range ($7°<2\vartheta<20°$), and at a distance L_1 from sample position.[17] The elastically exchanged wave vector Q is then evaluated from the measured neutron time of flight and diffraction angle 2ϑ.

We recorded neutrons diffracted from three samples (namely pure HCl, pure DCl and an isomolar mixture of HCl and DCl), condensed at the working thermodynamic conditions into a flat Ti–Zr container with an internal spacing of 2 mm and wall thickness of 1 mm; a similar container was already used for previous measurements performed on HBr and HI on SANDALS.[3,4] The lateral dimension of this container was 23 mm and it was fully bathed by the cylindrical shaped neutron beam ($\phi=32$ mm). The sample container was surrounded by a radiation shield of thin aluminum foil and mounted on a close cycle refrigerator, with two thermocouples and heaters attached to the top and bottom so that the temperature was controlled, within ± 0.2 K. Measurements on the three samples were performed on the orthobaric liquid at $T=(194\pm 0.2)$ K, $P=(4.5\pm 0.5)$ bar (state point 1) and $T=(313\pm 0.2)$ K, $P=(65.5\pm 0.5)$ bar (state point 2). Since the saturated vapor pressures for these two temperatures are 1.32 bar and 64 bar, respectively,[16] the experimental conditions guaranteed the liquid meniscus to be kept always above the top of the sample container during measurements. Diffracted neutrons were also recorded for the empty container, vanadium calibration sample and background. Several runs for each sample were recorded, each lasting roughly three hours, in order to check both the reproducibility and the stability of the experimental apparatus.

TABLE I. Neutron scattering lengths, b, scattering cross sections, σ_s, and absorption cross sections for 2200 m/s neutrons, σ_a, according to Ref. 20.

ELEMENT	b (fm)	σ_s (barn)	σ_a (barn)
H	−3.7406	82.03	0.3326
D	6.671	7.64	0.000519
Cl	9.577	16.8	33.5

B. Data analysis

The experimental time of flight data were corrected to account for detector efficiency, background, multiple scattering, attenuation and scattering from empty container, according to standard routine available on SANDALS, and following a reduction scheme described in detail in Ref. 18. Inelastic contributions in the differential scattering cross sections have been estimated, on the assumption that they are negligible for the interference term, following the procedure fully described in Ref. 19.

For each sample, α, eight interference scattering cross sections, $F_\alpha(Q)$, were derived, one for each group of scattering angles, and after checking their internal consistency these functions were merged together in order to improve statistics. This check guaranteed that the angle dependent systematic errors have been reliably accounted for. The interference function can be expressed in terms of the partial structure factors (PSF), $H_{ij}(Q)$, for the α-th sample as

$$F_\alpha(Q)=\sum_{ij} b_i b_j H_{ij}(Q), \tag{1}$$

where b_j is the neutron coherent scattering length of the j-th atomic species, averaged over the spin and isotope states of the nuclei. The b_j values and the scattering and absorption neutron cross-sections of the single nuclei of interest in this experiment are summarized in Table I.[20]

The $H_{ij}(Q)$ functions were derived for each thermodynamic point investigated by linearly combining the interference scattering cross sections for the three samples.

The partial structure factors contain information about the spatial arrangement of the atomic sites and indeed they are defined as Fourier transforms of the site-site radial distribution functions, $g_{ij}(r)$, through

$$H_{ij}(Q)=4\pi\rho\int_0^\infty r^2[g_{ij}(r)-1]\frac{\sin Qr}{Qr}\cdot dr. \tag{2}$$

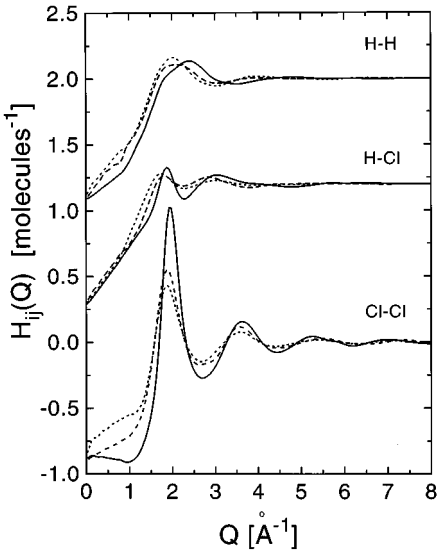

FIG. 1. The partial structure factors of HCl at state point 1 (solid line) and state point 2 (dotted line), compared with the data of Ref. 11 (dashed line). Notice that $H_{\mathrm{ClH}}(Q)$ has been shifted by $+1.2$ molecules^{-1}, and $H_{\mathrm{HH}}(Q)$ by $+2$ molecules^{-1}.

The $g_{ij}(r)$ functions were derived using the minimum noise reconstruction algorithm (MIN).[21] This data analysis procedure has been already adopted extensively in the analysis of previous experimental data, e.g., in HBr and water, and its advantages have been also fully described elsewhere.[4,19,21]

An Empirical Potential Monte Carlo (EPMC) simulation[8] was performed on the extracted radial distribution functions in order to produce three-dimensional configurations of HCl molecules compatible with the $g_{ij}(r)$ functions derived from the experiment. These have allowed the orientational correlations among neighboring molecules to be explored in greater detail, through the calculation of the angular pair correlation function, $g(\vec{r},\Omega_1,\Omega_2)$. Ω_1 and Ω_2 define the orientations of molecules 1 and 2 and $\vec{r}$ is the separation between their centers of mass. For an isotropic fluid of linear molecules $g(\vec{r},\Omega_1,\Omega_2)$ depends only on four independent variables, which may be chosen to be: the distance $r=|\vec{r}|$, the polar angle of vector $\vec{r}$, ϑ_L, and the polar and azimuthal angles of molecule 2 relative to molecule 1, namely ϑ_M and φ_M. Thus $g(r,\vartheta_L,\vartheta_M,\varphi_M)$ represents the probability that, given a molecule in the origin, oriented along $\vec{z}$, another molecule is found at a distance r, in the ϑ_L direction, with polar and azimuthal angles equal to ϑ_M and φ_M, respectively.

III. RESULTS AND DISCUSSION

A. Partial structure factors

In Fig. 1 the three PSF for $T=194$ K and $T=313$ K are reported, along with the data from Ref. 11 ($T=297$ K), with the aim of pointing out the effects of density and temperature (both change by $\sim 40\%$). In all three PSF peaks below 5 Å^{-1} become sharper and move towards higher Q-values, as the melting point is approached. We also find an excellent overall agreement between earlier results by Soper and Egelstaff[11] and our data at the highest temperature (state point 2): the small differences being likely ascribable to the different thermodynamic conditions and to the worse statistics of the earlier data. As an additional comment we note that the first peak of the $H_{\mathrm{HH}}(Q)$ function at the lowest temperature shows a shoulder at its left hand side. A similar feature, absent in liquid HI,[3] was already observed in liquid HBr[4] at the same reduced temperature. The comparison of these experimental results with the predictions for a model liquid with uncorrelated molecular orientations, as reported in Refs. 3 and 4, shows that the position of this shoulder coincides with the position of the first peak of the model liquid simulation. In HCl at the higher temperature states the first peak of the HH PSF is found to recover the shoulder position. This could imply that the distortions of the hydrogen–hydrogen PSF with respect to the model liquid increase with the quadrupole moment and lowering the temperature along the coexistence curve.

B. Intermolecular site-site correlation functions

In Fig. 2 the three intermolecular site-site correlation functions for liquid HCl are plotted for both thermodynamic points. We observe that in all three functions the peaks appear more pronounced and defined at state point 1, as expected. In particular in going from state point 1 to state point 2 the first peak of the $g_{\mathrm{Cl-Cl}}(r)$ correlation function [Fig. 3(a)] broadens but its position does not apparently change, whereas the second and third peak shift towards higher r-values. As a consequence above room temperature the $g_{\mathrm{Cl-Cl}}(r)$ correlation function shows very similar features to those generally displayed in a monatomic fluid: a sharp first peak followed by a second peak centered at about twice the position of the first one. These characteristics are reproduced by the calculations of Ref. 15.

The $g_{\mathrm{ClH}}(r)$ functions are plotted in Fig. 2(b). In this case we note that at state point 1 the correlation function exhibits three well defined peaks, the first one centered at about 2.4 Å, the main one at about 4.5 Å and the third one at about 7.5 Å. Going from state point 1 to state point 2 these peaks shift towards higher r-values and in the r-range between 5 Å and 7.5 Å the whole pair correlation function exhibits a strong change in the amplitude of the oscillations. The major changes with the thermodynamic state are, however, observed between 1.8 Å and 3.5 Å, i.e., in the region where the hydrogen bonded molecules have been suggested to contribute.[10,12] The peak centered at ~ 2.4 Å shifts to ~ 2.6 Å as the temperature increases and the density decreases; we notice that in the data reported in Ref. 11 this peak appears as a shoulder of the main second peak, due to the lower resolution. A similar trend of the so called hydrogen bond peak has been recently observed in high temperature water.[22,23]

A similar strong change with the thermodynamic state is also observed in the $g_{\mathrm{HH}}(r)$ function, Fig. 2(c), where the first peak shifts from about 3.1 Å at state point 1 to 3.7 Å at

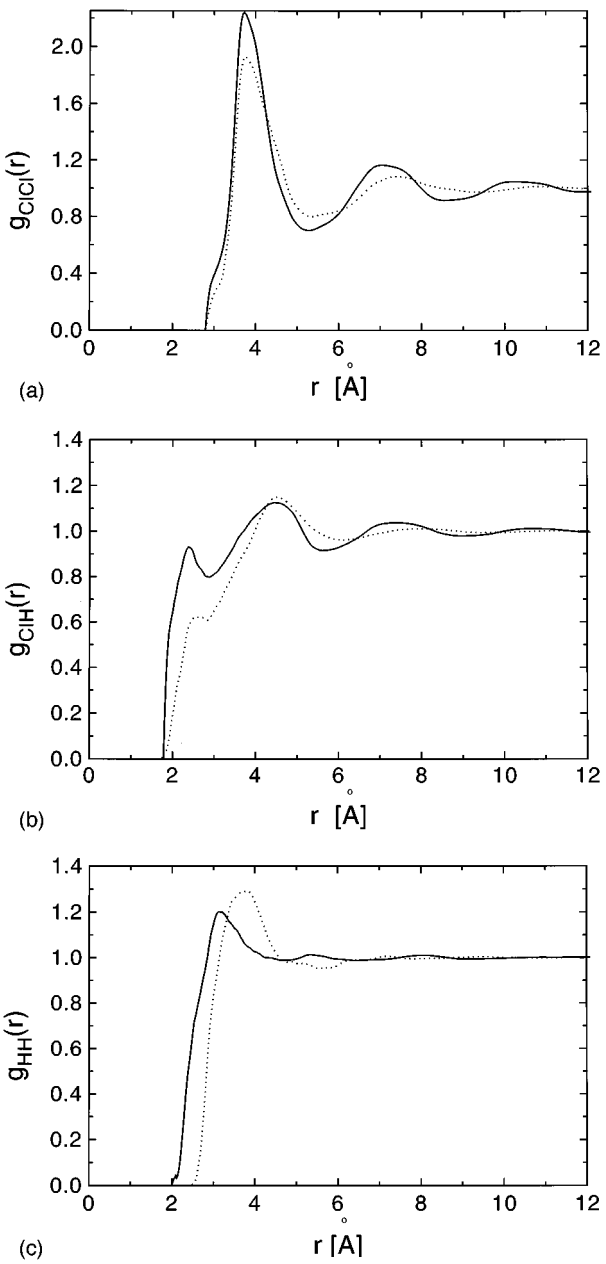

FIG. 2. The site-site radial correlation functions at state point 1 and 2 (same symbols as in Fig. 1): (a) $g_{\mathrm{ClCl}}(r)$, (b) $g_{\mathrm{ClH}}(r)$, (c) $g_{\mathrm{HH}}(r)$.

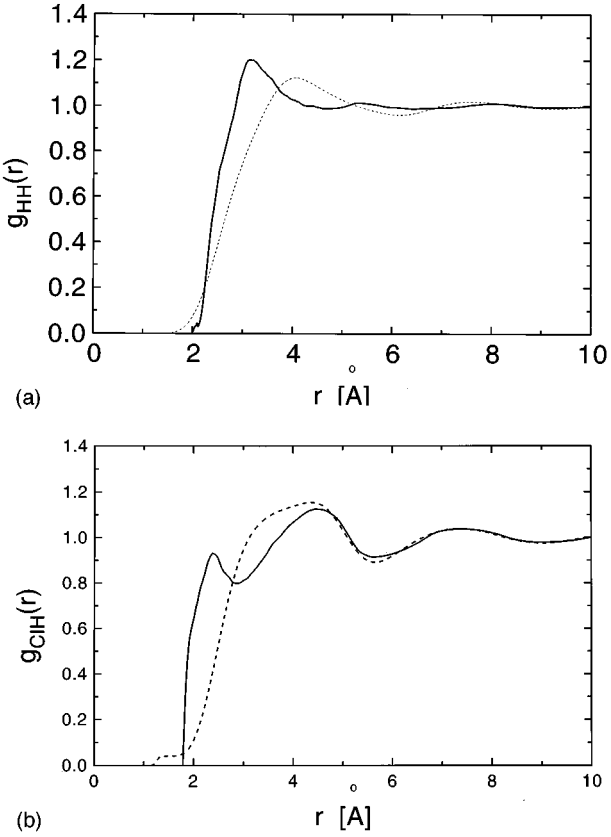

FIG. 3. Comparison of the experimental site-site radial correlation functions of HCl at state point 1 (solid line) with the predictions for an equivalent orientationally uncorrelated liquid (dashed line): (a) $g_{\mathrm{HH}}(r)$, (b) $g_{\mathrm{ClH}}(r)$.

state point 2. At state point 1 a peak at $\sim$5.3 Å is also visible.

A feature common to all three $g_{ij}(r)$ functions is the relaxation of the long range order, going from state point 1 to state point 2.

Figure 3 shows the comparison of the $g_{\mathrm{HH}}(r)$ and $g_{\mathrm{ClH}}(r)$ functions extracted at state point 1 with the prediction for a HCl liquid where molecules have the same center-center (Cl–Cl) distribution as the present data, but where the molecules are orientationally uncorrelated. The model has been exhaustively described in previous papers[3,4] and already compared with the experimental results for liquid HI and HBr. Here it should be noted only that while the $g_{\mathrm{HH}}(r)$ is sensitive to orientational correlations between the molecular axes and between the intermolecular vector and the molecular axis, the $g_{\mathrm{ClH}}(r)$ function contains information on orientational correlations between the intermolecular vector and molecular axis only. Both Fig. 3(a) and Fig. 3(b) are evidence for strong orientational correlations in liquid HCl. In particular we find the same qualitative disagreement between the experimental data and the model for the HH partial correlation functions of the three hydrogen halides studied so far: the experimental $g_{\mathrm{HH}}(r)$ function is more structured and its first peak appears at shorter distances than predicted for the uncorrelated liquid. More interesting is the result found for the correlations between molecular axis and intermolecular vector: these are indeed rather strong in liquid HCl, contrary to what is found in the other two hydrogen halides,[3,4] as shown by the presence in Fig. 3(b) of a well defined peak at about 2.4 Å, which is absent both in the predictions for the uncorrelated liquid and in the experimental data for the other two liquids. The evolution of the above correlations as a function of the dipole moments in liquid hydrogen halides can be appreciated by looking at Fig. 4. In this figure the $g_{XH}(r)$ functions for HCl, HBr, and HI are compared after scaling the r-axis by the Lennard-Jones diameter of the corresponding halide atom.[11,4,3] We note that whereas the long range order and the main peak at $\sim r/\sigma_{XX}=1.3$ are brought

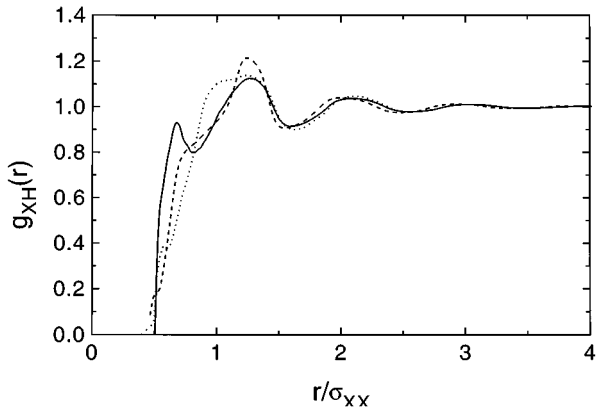

FIG. 4. The halide-hydrogen radial correlation functions of HCl (solid line), HBr (dashed line) and HI (dotted line) at a reduced temperature $T/T_c=0.6$. The x-axis coordinate has been reduced using the effective Lennard-Jones diameter for the halide atom quoted in Refs. 11, 4, and 3, respectively.

into coincidence by the rescaling, below $r/\sigma_{XX}=1$ the shoulder seen in HI evolves towards a clear peak in HCl.

C. EPMC analysis

The EPMC simulation has been performed for both the present data set and for the data of Ref. 11. Figure 5 shows the $g(r,\vartheta_L,\vartheta_M,\varphi_M)$ for state point 1 averaged over ϑ_M and φ_M, hereafter denoted as $g(r,\vartheta_L)$, which represents the probability that, given a molecule in the origin, oriented along the $\vec{z}$ axis, another molecule, however oriented, is found at a distance r in the direction ϑ_L. We notice that the radial correlation function of the molecular centers of mass can be obtained by averaging this function over ϑ_L: since in HCl the center of mass is almost coincident with the Cl site, this average coincides also with the $g_{\mathrm{ClCl}}(r)$ function, as already pointed out. Two shells of neighbors are identified in Fig. 5: the first at $r\sim3.5$ Å and the second at $r\sim6.5$ Å. Similar maps although with broader peaks are obtained at the other two state points. Since the position of the two peaks does not change with ϑ_L, the $g_{\mathrm{ClCl}}(r)$ function will exhibit peaks at roughly the same positions [see Fig. 2(a)]. The function $g(r,\vartheta_L)$ shows a strong dependence on ϑ_L at r values close to the first neighboring shell, indicating, contrary to what would be expected for an uncorrelated model liquid, a clear preferred orientation of the intermolecular axis within a cone of half width $\vartheta_L=50°$. In other words, while the preferred distance of the first neighboring molecules around an oriented molecule is the same in all ϑ_L directions, they are not isotropically distributed, since they prefer to lie in the axial direction. It is worthwhile noticing that, since the Cl site is close enough to the molecular center of mass, also the

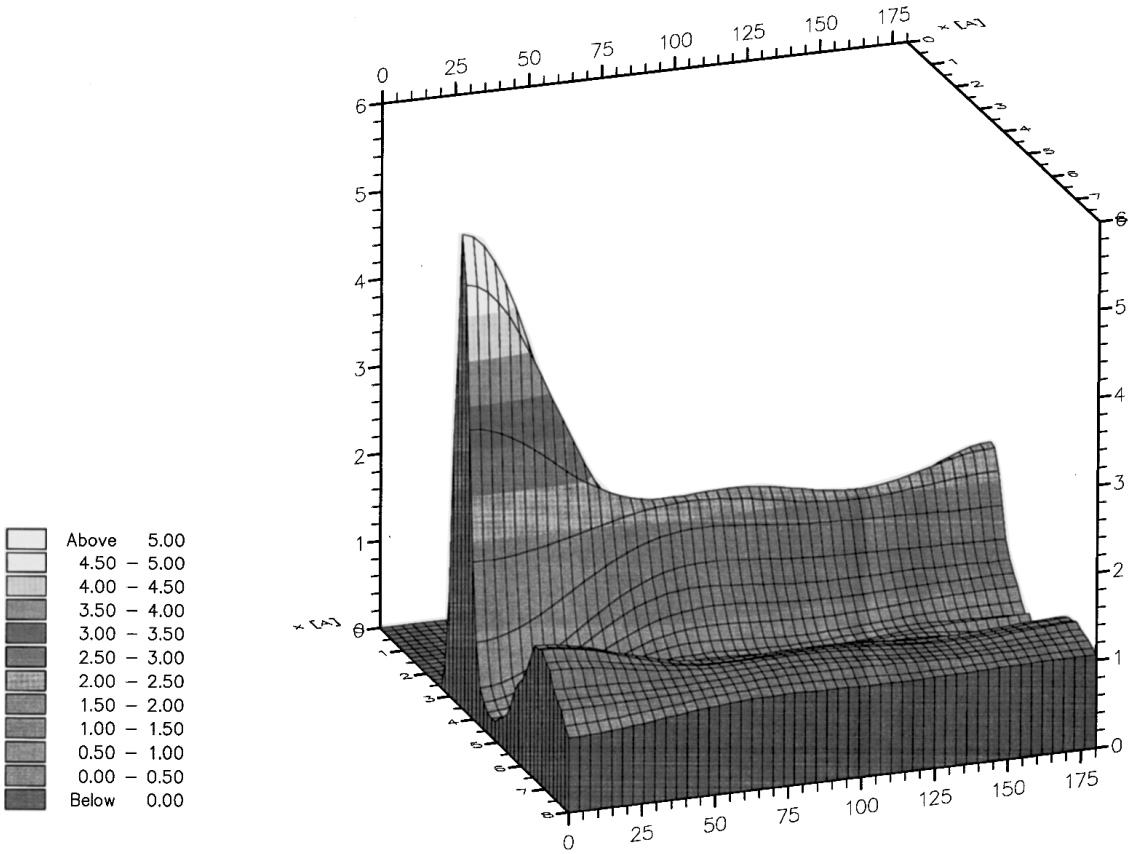

FIG. 5. Map of the of the probability, $g(r,\vartheta_L)$, that, given a central HCl molecule in the origin, oriented along the $\vec{z}$ axis, another molecule, however oriented, is found at a distance r in the direction ϑ_L, at state point 1.

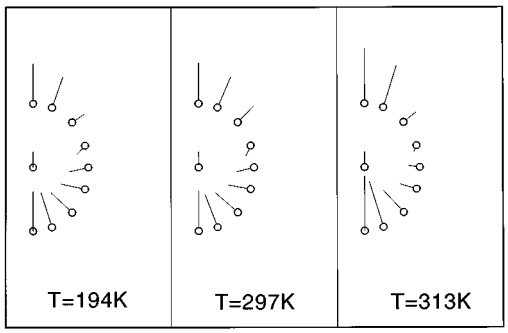

FIG. 6. Schematic representation of the results of the EPMC analysis of the present NDIS data and of the previous ones.[11] The first molecule is in the origin with the Cl site represented by an open circle and the H site pointing towards the $\vec{z}$ axis direction. Its first neighboring molecules are represented by an open circle at the Cl site, with a bar oriented along the preferred ϑ_M direction at each ϑ_L value considered. The length of the bars is roughly proportional to the maximum of the probability function $g(r,\vartheta_M|\vartheta_L)$.

$g_{\mathrm{ClH}}(r)$ function is determined by an appropriate average of $g(r,\vartheta_L)$, keeping fixed the distance between the H and Cl sites. Thus deviations from the uncorrelated model results, and in particular the existence of the H-bond peak, depend on the strong directionality observed in the first neighbors distributions.

From the EPMC simulation we have also calculated the average of $g(r,\vartheta_L,\vartheta_M,\varphi_M)$ over φ_M, at nine selected ϑ_L values (namely 0°, 20°, 45°, 70°, 90°, 110°, 135°, 160°, 180°), hereafter referred to as $g(r,\vartheta_M|\vartheta_L)$. This function represents the probability that, given a molecule at the origin, oriented along the z axis, another molecule lies at a distance r, in the direction ϑ_L, with orientation defined by the polar axis ϑ_M. The results obtained at the nine ϑ_L values considered are drawn schematically in Fig. 6 for all three state points. The molecules are represented by bars and the chlorine site is labelled by a circle; the molecule in the origin is oriented parallel to the $\vec{z}$ axis and the second molecules along the preferred ϑ_M direction at each ϑ_L value. The relative length of the second molecules is proportional to the maximum height of the density distribution. We notice that at all state points the majority of the first neighboring molecules, which lie in a region where $0\leqslant\vartheta_L\leqslant 20°$ or $160°\leqslant\vartheta_L\leqslant 180°$, as already seen from Fig. 5, have their dipoles almost aligned: this tendency becomes more evident going from state point 1 to state point 2. Very few L-shaped configurations are found at $\vartheta_L\simeq 90°$, where, however, a preferred relative orientation of molecules is hardly detectable. This analysis confirms the existence of strong correlations between the intermolecular vector and the molecular axis, suggested in the previous section by the comparison with the uncorrelated liquid model. A closer look at the preferred orientations at $\vartheta_L=0°$ is given in Fig. 7, where the function $g(r,\vartheta_M|\vartheta_L=0)$ at state points 1 and 2 is reported. At state point 1, although first neighboring molecules seen along the positive $\vec{z}$ direction strongly prefer to align their dipole parallel to the dipole of the molecule at the origin, significant density of molecules is also found at $\vartheta_M\sim 70°$, while no antiparallel dipole orientations are found. The angular distribution sharpens on going to state point 2, indicating a better alignment of the dipole moments at the lower density state, while the intensity of the shoulder at $\vartheta_M\sim 70°$ decreases, and only a few antiparallel configurations appear.

The EPMC analysis of the HCl data gives strongly different results in comparison with those found by the spherical harmonics analysis of the HI[21] and HBr[4] data. In those liquids the correlation between ϑ_L and the molecular orientation was found to be very low, with the majority of the molecules forming an angle $\vartheta_M=45°$ with the $\vec{z}$ direction and almost the same number of parallel and antiparallel dipoles. These differences may be due to the different dipole and quadrupole moments associated with the three molecules or to the presence in liquid HCl of hydrogen bonds, which implies stronger directionality in the local coordinations. However, it should be kept in mind that previous data on hydrogen halides have been analyzed with a rather different technique. In order to make a more quantitative estimate of the degree of hydrogen bonding in liquid HCl it will be necessary to distinguish between electrostatic effects which lead to a simple alignment of dipoles, and true hydrogen bonding effects which will probably lead to different near-neighboring orientations. Because the Cl–H bond direction coincides with the HCl dipole moment direction, a suitable geometric definition of the H-bond in this system is not available at the present time, unlike the case of liquid water where the O–H bond direction is distinct from the water molecule's dipole moment direction. Therefore further analysis of the degree of hydrogen bonding in HCl is postponed to a later study where the degree of orientational correlation in HCl, HBr, and HI will be compared. What is clear already, however, is that there appear to be competing dipolar and hydrogen bonding interactions in HCl, and as the temperature is raised and the density is lowered the dipolar interactions tend to dominate the structure.

IV. CONCLUSIONS

In summary we have achieved for the first time a detailed description of the microscopic structure of liquid HCl along the coexistence curve. Although strong orientational correlations are present at all states investigated, the radial distribution function of molecular centers is similar to that found in so called ''simple liquids.'' This is evident from Fig. 2(a) and from the independence of the position of the first neighbor peak of $g(r,\vartheta_L)$ on the ϑ_L coordinate. This finding implies that the short range electron overlap forces in liquid HCl are spherically isotropic.

Electrostatic and hydrogen bonding forces must therefore be primarily responsible for the observed orientational correlations. These correlations are characterized by a strongly anisotropic angular distribution of first neighboring molecules, which is markedly peaked around $\vartheta_L=0°$ (see Fig. 5). First neighboring molecules along this direction prefer to align their dipoles parallel to the molecule at the origin, although, at the lowest temperature also, a relevant fraction of molecules forming an angle $\vartheta_M\simeq 70°$ with the

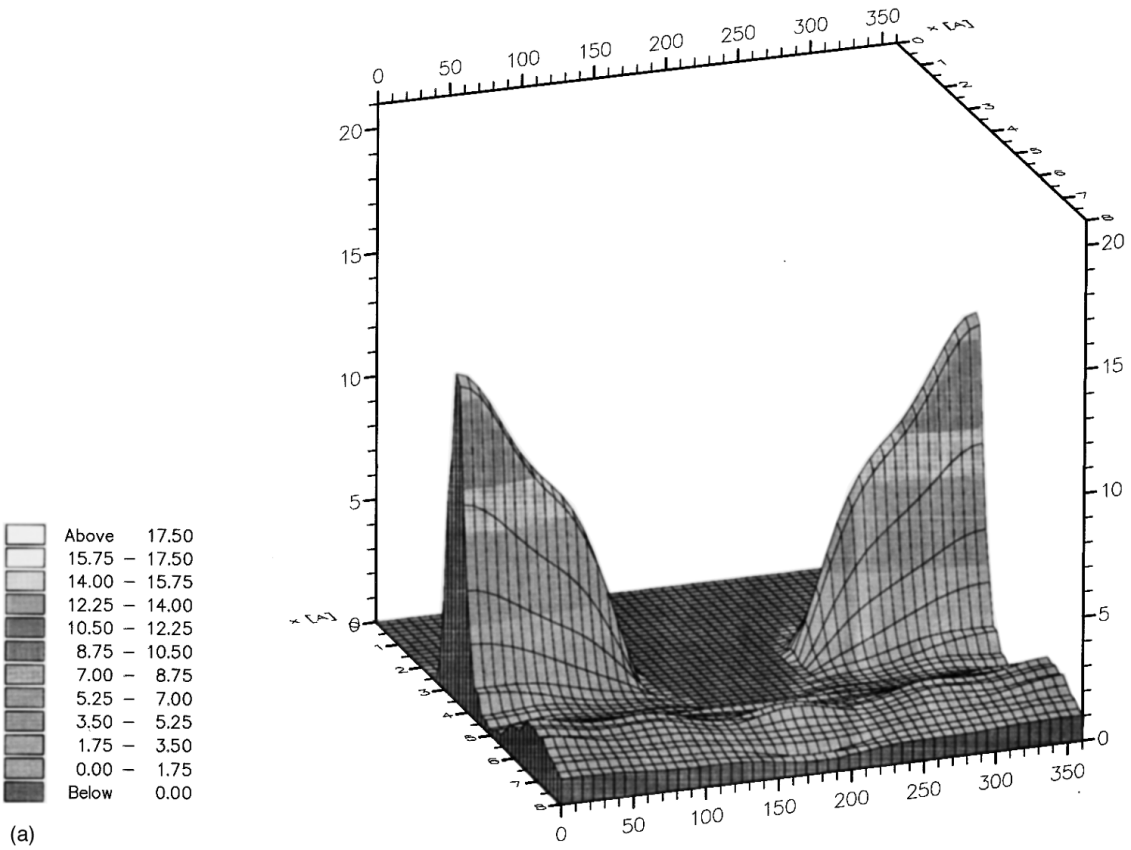

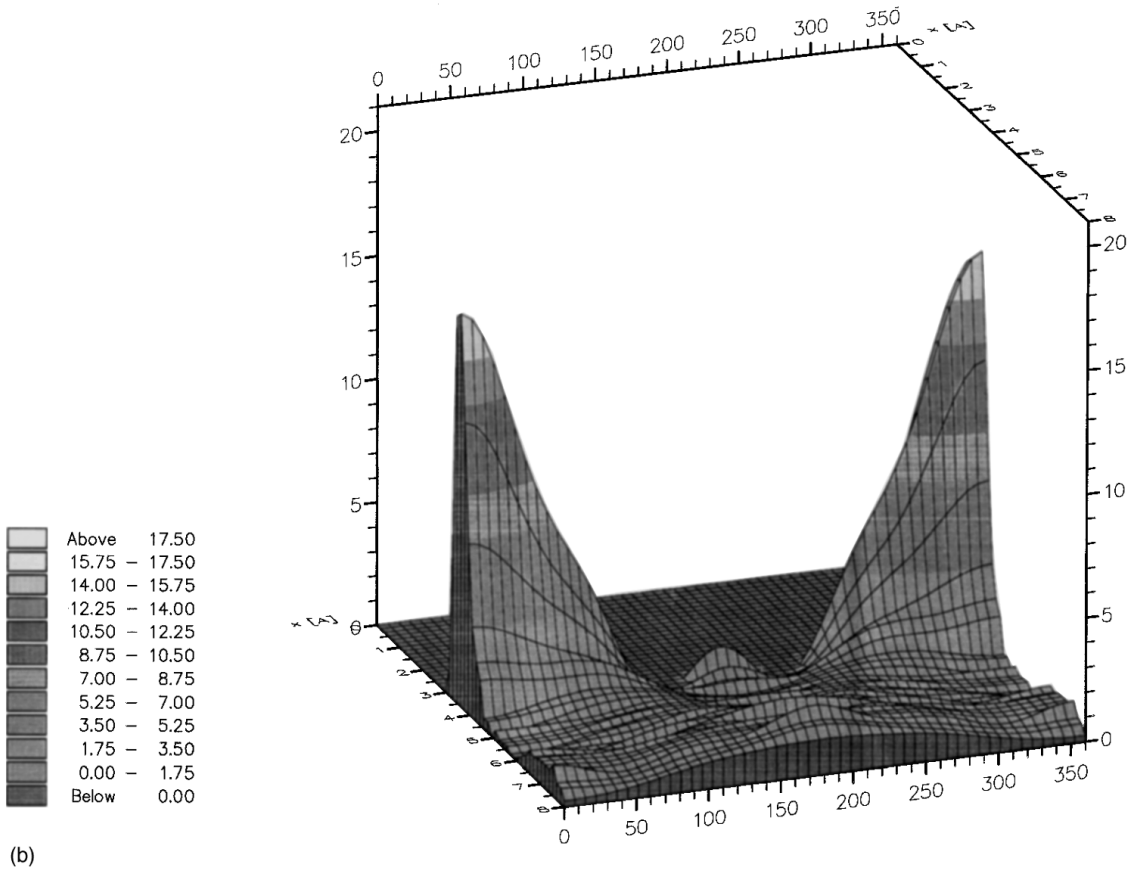

FIG. 7. Map of the probability, $g(r, \vartheta_M | \vartheta_L = 0°)$, that, given a central HCl molecule in the origin, oriented along the $\vec{z}$ axis, another molecule lies at a distance r, in the direction $\vartheta_L = 0°$, with orientation defined by ϑ_M: (a) $T = 193$ K; (b) $T = 313$ K.

molecule at the origin is found (see Fig. 7). We believe that these molecules are those engaged in hydrogen bonds. Going towards the critical point the number of these molecules decreases in favor of those with parallel orientation. This assignment is supported by the evidence for zig-zag structures with $\vartheta_M \simeq 87°$ in the crystalline forms of HCl[24] and by its dependence on the thermodynamic state. As already pointed out, the presence of hydrogen bonds is traditionally associated with the presence of a peak at $r \simeq 2.4$ Å: this peak is indeed present in our data. The behavior of its intensity is consistent with that of the number of first neighboring molecules around $\vartheta_L = 0°$, forming an angle $\vartheta_M \simeq 70°$.

We stress that liquid HCl looks different from the other hydrogen halides studied so far, because in the other two systems no evidence was found for the presence of hydrogen bonds and the correlations between the intermolecular vector and the molecular orientations were also very weak.[3,4,21]

It is the intention now to analyze all the existing data on HI,[3] HBr[4] and HCl using the same (EPMC) computer simulation technique used here. This will serve to highlight the changes in the liquid structure along the hydrogen halide series and so elucidate the extent to which this series can be regarded as hydrogen bonded.

Finally we note that the potential model proposed in Ref. 15 seems to reproduce the density dependence of the $g_{\mathrm{ClH}}(r)$ function and the ''simple liquid'' appearance of $g_{\mathrm{ClCl}}(r)$ at supercritical states. Thus it would be worthwhile to test this potential against our data.

ACKNOWLEDGMENTS

These experiments would not have been possible without the continued technical support from J. Dreyer and his staff at ISIS. The financial support of the C.N.R. is gratefully acknowledged.

[1] S. W. Lovesey, *Theory of Neutron Scattering from Condensed Matter* (Clarendon, Oxford, 1984), Vol. 1.
[2] A. K. Soper, in *Methods in the Determination of Partial Structure Factors*, edited by J. B. Suck, D. Raoux, P. Chieux, and C. Riekel (World Scientific, London, 1993), p. 58.
[3] C. Andreani, M. Nardone, F. P. Ricci, and A. K. Soper, Phys. Rev. A **46**, 4709 (1992).
[4] C. Andreani, F. Menzinger, M. A. Ricci, A. K. Soper, and J. Dreyer, Phys. Rev. B **49**, 3811 (1994).
[5] C. G. Gray and K. E. Gubbins, *Fundamentals, Theory of Molecular Liquids* (Oxford University Press, New York, 1984), Vol. 1.
[6] R. L. McGreevy and M. A. Howe, Ann. Rev. Mater. Sci. **22**, 217 (1992).
[7] M. P. Allen and D. J. Tildesley, *Computer Simulation of Liquids* (Oxford University Press, Oxford, 1987).
[8] A. K. Soper, Chem. Phys. **202**, 295 (1996).
[9] C. Andreani, F. Menzinger, M. Nardone, F. P. Ricci, M. A. Ricci, and A. K. Soper, in *Hydrogen Bond Networks*, edited by M. C. Bellissent-Funel and J. Dore, NATO ASI Series, Series C **435**, 113 (Kluwer, Dordrecht, 1993).
[10] J. G. Powles, E. K. Osae, J. C. Dore, and P. Chieux, Mol. Phys. **43**, 1051 (1981).
[11] A. K. Soper and P. A. Egelstaff, Mol. Phys. **42**, 399 (1981).
[12] T. Bausenwein, H. Bertagnolli, K. Todheide, and P. Chieux, Ber. Bunsenges. Phys. Chem. **95**, 577 (1991).
[13] J. G. Powles, W. A. B. Evans, E. McGrath, K. E. Gubbins, and S. Murad, Mol. Phys. **38**, 893 (1979).
[14] M. L. Klein and I. R. McDonald, Mol. Phys. **42**, 243 (1981).
[15] D. Gutwerk, T. Bausenwein, and H. Bertagnolli, Ber. Bunsenges. Phys. Chem. **98**, 920 (1994).
[16] *International Critical Tables*, Vol. III, p. 228.
[17] A. K. Soper, in *Proceedings of the Conference on Advanced Neutron Sources 1988*, edited by D. K. Hyer, IOP Conf. Proc. No. **97** (Institute of Physics and Physical Society, London, 1989), p. 353.
[18] A. K. Soper, W. S. Howells, and A. C. Hannon, Rutherford Appleton Laboratory Report No. 89-046, 1989 (unpublished).
[19] P. Postorino, M. A. Ricci, and A. K. Soper, J. Chem. Phys. **101**, 4123 (1994).
[20] V. F. Sears, Neutron News **3**, 26 (1992).
[21] A. K. Soper, C. Andreani, and M. Nardone, Phys. Rev. E **47**, 2598 (1993).
[22] F. Bruni, M. A. Ricci, and A. K. Soper, Phys. Rev. B **54**, 11876 (1996).
[23] A. K. Soper, F. Bruni, and M. A. Ricci, J. Chem. Phys. **106**, 247 (1997).
[24] *Comprehensive Inorganic Chemistry*, edited by J. C. Bailar, H. J.Emeleus, Sir Ronald Nyholm, and A. F. Trotman-Dickenson (Pergamon, Oxford, 1974).